Absence of anomalous dispersion features in the inelastic neutron scattering spectra of water at both sides of the melting transition

F.J. Bermejo
Instituto de Estructura de la Materia, Consejo Superior de Investigaciones Científicas, Serrano 123, E-28006 Madrid, Spain

M. Alvarez*
Department of Neutron Physics, Royal Institute of Technology, S-100 44 Stockholm, Sweden

S.M. Bennington
ISIS Pulsed Neutron Facility, Rutherford Appleton Laboratory, Chilton, Didcot, Oxon OX11 0QX, United Kingdom

R. Vallauri
Dipartimento di Fisica, Università degli Studi di Trento, I-38050 Povo-Trento, Italy
(Received 13 July 1994; revised manuscript received 7 September 1994)

Inelastic neutron scattering spectra of water a few degrees below and above melting have been measured. The excitations seen in the hot solid are analyzed in terms of the wave vector dependence of the average frequencies characterizing the envelopes of the *mostly* acoustic and *mostly* optical manifolds, which are confined to energy transfers below 40 meV. The spectra corresponding to the liquid are analyzed by means of a model which includes stochastic, zero-frequency motions (long range translational and rotational diffusion) using the values for the relevant transport coefficients measured under high-resolution conditions. The excitation frequencies in the solid and liquid phases follow a behavior common to other molecular liquids examined so far, approaching hydrodynamic sound at low momentum transfers.

PACS number(s): 61.20.−p, 64.70.−p

I. INTRODUCTION

The possible existence of strong anomalous dispersion in the propagation of collective excitations in liquid water, evidencing phase velocities well above those characteristic of hydrodynamic sound, has been a recurrent theme since the very first discussion about this topic by Rahman and Stillinger [1] based upon results derived from molecular dynamics (MD) calculations of the $S(Q,\omega)$ dynamic structure factor. A flurry of (mostly) numerical results followed from computer simulations, some of them motivated by suggestions made on the basis of kinetic-theory results [2], which predicted the existence of "fast sound" modes in systems composed by particles of disparate masses. The aims of such efforts thus were to confirm or reject the presence of such anomalously fast modes visible within the kinematic regime accessible to computer molecular dynamics simulation and inelastic neutron scattering (INS), as well as to clarify its relationship with hydrodynamic sound. Two different interpretations were then proposed to explain the apparently large values for the sound velocity derived from simulational means, stating in the first case [3] the existence of two different collective modes observable at low and large wave vectors, respectively, whereas others (i.e., Wojcik and Clementi and Sciortino and Sastry in Ref. [2]) postulated the continuity of those collective excitations, passing from hydrodynamic sound to the high-frequency mode by means of some strong positive dispersion very much akin to that observed in simple, monoatomic liquids. In contrast, very scarce experimental results have appeared regarding this topic, with the exception of preliminary measurements by Teixeira *et al.* [3], where the presence of such anomalous excitation could not be proved convincingly (i.e., the results are strongly dependent upon the model used to analyze the inelastic intensities). To add further complication, the measured results could not be referred to those occurring at the other side of the melting transition due to the lack of experimental data regarding the hot crystal. As a matter of fact, to the authors' knowledge, the only set of dispersion curves for single-crystal ice *Ih* which has appeared in the literature is that of Renker [4] measured a long time ago, although some recent progress has been registered regarding the accurate measurements of the vibrational densities of states at low temperatures of solid water in several phases (hexagonal and cubic ices as well as low- and high-density amorphous phases) [5]. The dearth of experimental neutron data regarding the study of excitations in the ice *Ih* solid is attributable to the difficulties which arise from the underlying proton disordered lattice, something which substantially complicates the assignment of the inelastic intensities following

*Permanent address: Instituto de Química Física Rocasolano, CSIC, Serrano 119, E-28006 Madrid, Spain.

the traditional molecular Born–von Kármán route, since a substantial contribution to the intensities comes from a diffuse background [6].

Some recent works on the dynamics of polycrystalline ice [7,8] carried out at relatively low temperatures, while confirming the existence of inelastic signals with an apparently large velocity dispersion, also gave a microscopic explanation of the origin of such a feature. As shown in Fig. 2 of Ref. [7], two well separated branches of excitations are seen in the calculated $S(Q,\omega)$ dynamic structure factor for the ice (harmonic) polycrystal, within the frequency range usually assigned to translational motions in the $Z(\omega)$ (i.e., up to 40 meV, $\approx$ 10 THz) generalized frequency distribution (density of vibrational states). A plot of the maximum frequency of such manifolds versus momentum transfers revealed the acoustic character of the excitations grouped below the envelope of low frequencies, whereas that corresponding to higher frequencies was found to be strongly reminiscent of those reported from MD simulations in the liquid phase. In common with some other molecular materials studied so far [9], the origin of the higher-frequency excitations was found to be crystal modes with strong translational-rotational character, showing nonzero frequencies at low wave vectors (i.e., excitations of "optical" character). The fact that such an anomalously high value for the apparent phase velocity of the excitations has been found in MD simulations using very different thermodynamic conditions and interaction potentials could then easily be explained from the above considerations, and also from the fact that the quantity which is customarily plotted, $\omega_{max}(Q)$, is the frequency corresponding to the maximum of $J_l(Q,\omega) = \omega^2 S(Q,\omega)/Q^2$ (i.e., the longitudinal current-current correlation function), where, in the liquid phase, the low-frequency envelope only contributes as an ill-defined shoulder at low frequencies [10].

The aim of this paper is thus to provide experimental evidence regarding the collective dynamics in water at both sides of the freezing point. Such an exercise enables a comparison between the characteristic excitations in the hot solid and those in the liquid within a narrow range of temperatures so that most of the differences between the spectra corresponding to the different phases have to be attributed to the loss of long-range translational order. The present work thus complements that already reported [7,8] which was entirely focused on the study of polycrystalline ice at low temperatures, and provides an experimental benchmark which can be used in the future to contrast the results of MD simulations, and thus to improve the interparticle potential models employed there.

II. EXPERIMENTAL AND DATA ANALYSIS DETAILS

A. Experiment

The neutron measurements reported in this paper were carried out using MARI, a direct geometry chopper spectrometer located at one of the beam lines of the ISIS pulsed neutron facility, Rutherford Appleton Laboratory (Oxon, U.K.). The incident energy was set to 78.6 meV in order to cover a reasonable kinematical range at low wave vectors without degrading substantially the resolution in energy transfers. The achieved energy resolution was of about 1 meV, estimated from the vanadium-standard-sample runs as the half-width at half maximum (HWHM) of the elastic peak. Such kinematic conditions are to be compared with those of the previous experiment [3], which employed basically the same incident energy (79.6 meV) but the achieved resolution in energy transfers (2.38 meV) was substantially poorer. From previous experience with thermal triple-axis spectroscopy for a variety of molecular liquids [11], the effect of degrading the instrumental resolution to such an extent translates into substantial changes in the line shapes which become difficult to compare with those measured under higher-resolution conditions unless such windowing effects are removed by some means such as deconvolution [12]. As a matter of fact, convolution of the model scattering functions with a resolution function of the same width as that used by Teixeira *et al.* [3] will result in strongly distorted line shapes so that a substantial part of the scattering appears as inelastic to the naked eye. The sample (99.9% deuterated water) was contained in a holder consisting of two concentric thin walled aluminum cans of annular section (particularly suitable for the vertical arrangement of the detector banks on MARI) of dimensions 4.9 cm and 4.1 cm, as outer and inner diameter, respectively, and 6.3 cm of length. The free space between both cylinders was filled with the liquid sample through capillary tubing connected to an external reservoir. The temperature was controlled by means of a closed circle refrigerator which circulated a cryogenic mixture.

The measurements were carried out at two temperatures, right below ($T \approx 270$ K in the hexagonal Ih ice phase) and above ($T \approx 280$ K in the liquid phase) the melting point under atmospheric pressure. Finally, a third set of data was taken with the empty cell in order to correct the scattering from the sample holder. In summary, the experiment consisted of four runs: two of them corresponding to the sample at two different thermodynamic states, another run with the empty container, and an additional one with a standard vanadium foil.

B. Correction procedures and data reduction

Before a reliable total observed intensity $I_{obs}(Q,\omega)$ is obtained, some corrections have to be done in order to remove spurious effects from the experimental thermal neutron time-of-flight spectra. The corrected experimental intensities could then be expressed as

$$I_{obs}(Q,\omega) = S(Q,\omega) \otimes R(Q,\omega), \tag{1}$$

where $S(Q,\omega)$ is the dynamic structure factor suitable to be analyzed in terms of physically meaningful models and the one to be determined in the end, and $R(Q,\omega)$ is the instrumental resolution function. The symbol $\otimes$ denotes the convolution of the two functions and Q and

ω are, respectively, the momentum and energy transfers.

The corrections to be done have to account for the following effects: multiple scattering, container scattering, and background. Before performing those corrections, the experimental double differential cross section $d^2\sigma(\varphi,\omega)/d\omega d\Omega$ (with φ being a fixed scattering angle and Ω the solid angle) was converted from (φ,ω) space to (Q,ω) space making use of MARI standard programs which essentially interpolate from the experimental data to a rectangular (Q,ω) grid.

In every thermal neutron scattering experiment the measured cross section includes both single- and multiple-scattering events. In order to isolate the single-scattering cross sections, the contribution of multiply scattered neutrons was evaluated by means of a computer simulation code. For this purpose the MSCAT program, based on a Monte Carlo simulation code developed by Bischoff and extended by Copley first and Verkerk and co-workers later [13] was employed. The program effectively simulates the current scattering experiment and calculates a total scattering function $S_t(Q,\omega) \simeq S_{ms}(Q,\omega) + S_{ss}(Q,\omega)$, where ms and ss denote multiple and single scattering. This computation requires a more or less precise knowledge of the model function for single-scattering events as input of the program. In this case, a set of smoothed experimental data themselves were used

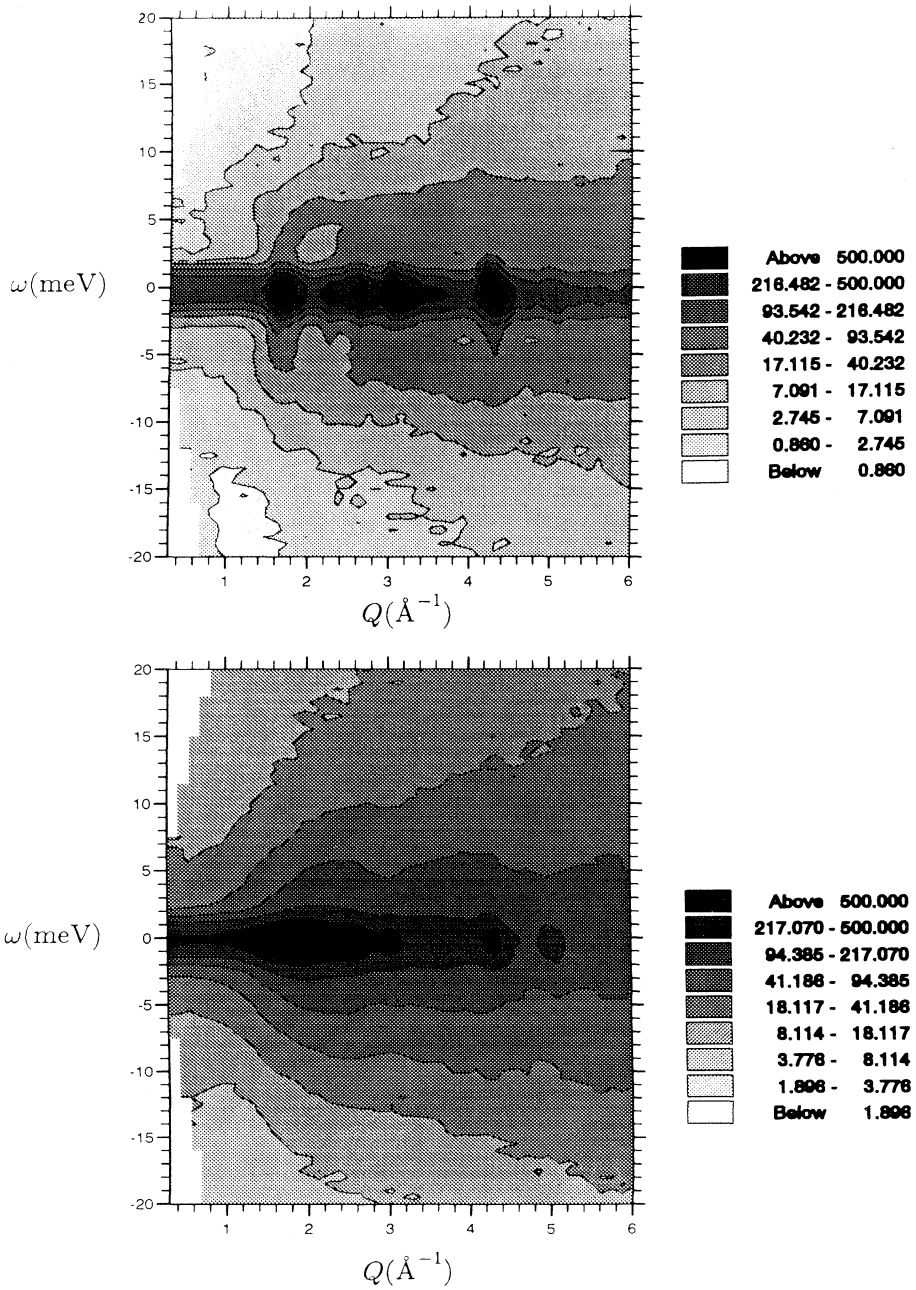

FIG. 1. Countour plots for the raw experimental intensities for D_2O ice Ih (upper frame) and water (lower frame). The scattered intensity is given in arbitrary units. Notice the asymmetry in the spectral distribution of ice as commented on in the text. The difference in scattering intensities between the solid and liquid can be attributed to the increased density in the liquid, as well as to the broadened quasielastic contribution.

as input to model $S_{inp}(Q,\omega)$. After removing the simulated multiple scattering, the resulting single-scattering contribution was taken as a new input, $S'_{inp}(Q,\omega)$. The iterative process stopped when $S'_{inp}(Q,\omega) \simeq S_{ss}(Q,\omega)$. Although an annular geometry is not explicitly taken into account by the program, we have run it considering our setup consisting of one empty cylinder sample container "made" of heavy water. The final multiple scattering was about 10% of the total intensity.

An empty can run was used to ground effects. Vanadium data allowed us to get a normalized $I_{obs}(Q,\omega)$.

A qualitative view of the differences between the frequency distributions between ice and liquid samples can be seen from contour plots of the raw intensities shown in Fig. 1. Well-defined finite-frequency features are seen in the graph corresponding to ice as a band of intensities going from ≈ 2 meV at $Q \approx 1.7$ Å^{-1} up to 6–7 meV for momentum transfers above 2.2 Å^{-1}. The asymmetry in the intensity distribution for energy-gain and -loss sides can be attributed to both the asymmetry in the instrumental resolution at low energies due to contamination with the moderator "storage term" and the detailed balance effects. Because of the strong elastic scattering of the crystals, the effects of such an asymmetry are particularly notorious for the solid and not so prominent for the liquid. In contrast, the plot regarding the liquid evidences a smoother behavior, and the existence of a clear inelastic response is inferred from the broad range of energy transfers covering substantial intensities (up to at least 20 meV). Also notice that if the observed response of the liquid were quasielastic in origin, a narrowing in the intensity distribution could be expected for wave vectors about the maximum of $S(Q)$, static structure factor, that is ≈ 1.8 Å^{-1} (de Gennes narrowing), whereas a behavior just opposite to that is observed in the referred plot.

C. Data analysis

The total intensity as derived after the correction procedures is given in terms of the coherent and incoherent contributions to the cross section as

$$I_{obs}(Q,\omega) = A\left[\left.\frac{d^2\sigma}{d\omega d\Omega}\right|_{coh} + \left.\frac{d^2\sigma}{d\omega d\Omega}\right|_{inc}\right] \otimes R(Q,\omega), \quad (2)$$

where A represents a global scaling constant. Since closed form expressions for the resolution function are difficult to derive for a chopper spectrometer, the estimate measured with the vanadium standard was used to approximate this quantity. The coherent and incoherent contributions to the cross section are then expressed in terms of the relevant dynamic structure factors as

$$\left.\frac{d^2\sigma}{d\omega d\Omega}\right|_{coh} = \sigma_{coh} S_{coh}(Q,\omega) = \sigma_{coh}\left[S^0(Q,\omega) + S^1(Q,\omega)\right], \quad (3)$$

$$\left.\frac{d^2\sigma}{d\omega d\Omega}\right|_{inc} = \sigma_{inc} S_{inc}(Q,\omega) = \sigma_{inc}\left[S_I(Q,\omega) + S_M(Q,\omega)\right], \quad (4)$$

where $\sigma_{coh,inc}$ stand for the coherent or incoherent cross section per molecule.

The coherent scattering has been approximated as resulting from two contributions, $S^0(Q,\omega)$ and $S^1(Q,\omega)$, which represent the zeroth- and finite-frequency contributions (one-phonon collective excitation). The modeling of the former term depends on whether the sample is in solid or liquid state, being in the first case the strictly elastic component of the structure factor [i.e., $S(Q,\omega=0)$]. In the case of the liquid state this term is modeled under the Sköld approximation from the respective incoherent scattering quantity which is described below. The inelastic scattering at nonzero frequencies comprised in Eq. (3) is modeled in terms of a damped harmonic oscillator (DHO) model [14]

$$S^1(Q,\omega) = H_Q\, n(\omega)\, \frac{4\,\omega\,\omega_Q\,\Gamma_Q}{(\omega^2 - \Omega_Q^2)^2 + 4\,\omega^2\,\Gamma_Q^2}, \quad (5)$$

with $n(\omega) = [1 - \exp(-\hbar\omega\beta)]^{-1}$ being the thermal occupation factor [$\beta = (k_B T)^{-1}$], ω_Q the oscillator bare frequency with a linewidth specified by the damping coefficient Γ_Q, and H_Q the strength of the single-phonon excitation. The physical frequency of such an oscillator is given by the renormalized quantity $\Omega_Q = (\omega_Q^2 + \Gamma_Q^2)^{1/2}$ and in the present case this quantity has to be interpreted, at least in the case of polycrystalline ice, as an average frequency corresponding to the center of gravity of the manifold of excitations under consideration. Also notice the fact that the damping coefficient Γ_Q gives a measure of the apparent broadening in terms of homogeneous and heterogeneous contributions, as arising from excitations of different frequencies which cannot be resolved and from finite-lifetime effects, respectively.

The terms regarding incoherent scattering given in Eq. (4) also have a somewhat different meaning depending upon the physical state of the sample. For the solid, the first term is given from the calculated $Z(\omega)$ [7], vibrational density of states, as

$$S_I(Q,\omega) = \frac{\hbar^2 Q^2}{2M_{mol}}\frac{Z(\omega)}{\omega}\{n(\omega)+1\}, \quad (6)$$

where M_{mol} was taken as the free-atom mass [i.e., $M_{mol} = (2\sigma_D\ M_D + \sigma_O\ M_O)/(2\sigma_D + \sigma_O)$, where the subscripts D and O identify the coherent cross sections of deuterium and oxygen, respectively]. A different approach is followed for the melt where these terms represent incoherent quasielastic scattering given by

$$S_I(Q,\omega) = S_{inc}^{quel}(Q,\omega) = \exp(-Q^2\langle u^2\rangle)\left[S_{trans}(Q,\omega) \otimes S_{rot}(Q,\omega)\right], \quad (7)$$

where $S_{trans}(Q,\omega)$ represents the contribution from the translational motion, which can be approximated with a random-jump-diffusion model by the Lorentzian

$$S_{trans}(Q,\omega) = \frac{1}{\pi}\frac{\Gamma_t(Q)}{\omega^2 + \Gamma_t^2(Q)}\ ,\ \Gamma_t(Q) = \frac{D_t Q^2}{1 + D_t Q^2 \tau_0}. \quad (8)$$

The low-frequency rotational motions of the molecules are approached in terms of the well-known Sears expansion [15] as follows:

$$S_{rot}(Q,\omega) = \sum_l (2l+1) j_l^2(Qa) \times \frac{l(l+1)\Gamma_r + \Gamma_t(Q)}{\omega^2 + [l(l+1)\Gamma_r + \Gamma_t(Q)]^2}. \quad (9)$$

All the parameters appearing in Eqs. (8) and (9) were taken from Ref. [16].

The term $S_M(Q,\omega)$ represents a multiexcitation contribution which, at these relatively high temperatures, becomes rather substantial at large wave vectors. For its computation, the Gaussian approximation [17] was followed. Notice that because of the high temperatures under consideration (i.e., no sharp features are visible even in the solid), as well as the substantial contributions from incoherent scattering ($\sigma_{coh}/\sigma_{inc} = 15.416/4.08$, i.e., approximately 21% of the total scattering), such approximation for multiphonon effects should be rather realistic. Explicitly, the contributions of multiexcitations are calculated as [17,18]

$$S_M(Q,\omega) = \exp[-2W(Q)] \frac{1}{\hbar\Lambda} \exp[\omega/\Lambda^2\gamma(0)] F(x,y),$$
$$x = \omega/\Lambda \ , \ y = 2W(Q) \exp\left(\frac{-1}{2\Lambda^2\gamma^2(0)}\right), \quad (10)$$
$$F(x,y) = \sum_{n=2}^{\infty} \frac{y^n}{n!} \frac{\exp(-x^2/2n)}{\sqrt{2\pi n}},$$

where the quantities $W(Q)$, Λ, and $\gamma(0)$ are calculated, in the case of polycrystalline ice, from the $Z(\omega)$ density of states given in a previous paper, and from the same quantity derived from MD simulations [1] for the melt

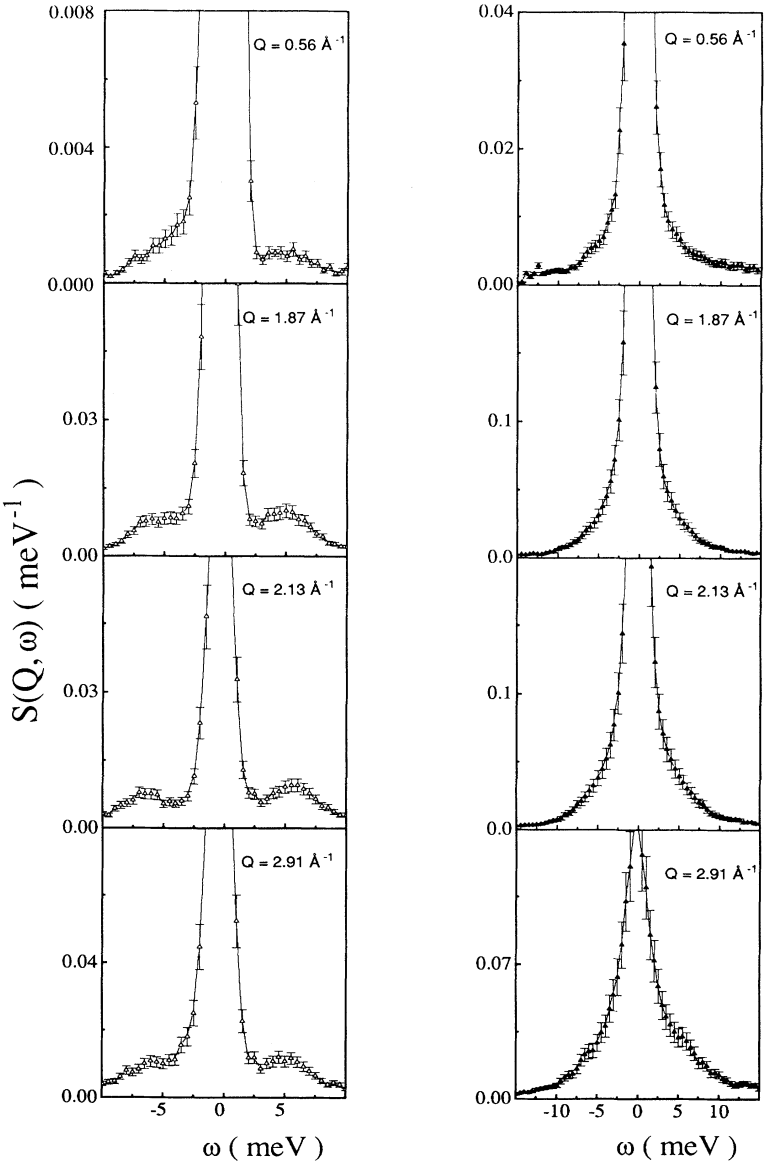

FIG. 2. The left column (open triangles) shows constant-Q spectra for the solid, for wave vectors below (0.56 Å^{-1}), about the maximum of the first Bragg reflection (1.87 Å^{-1}), and well above it. The column at the right hand side (filled triangles) shows the spectra of water for the same values of the momentum transfer. Solid lines joining the experimental points are guides to the eye.

according to

$$\gamma(0) = \frac{\hbar^2}{2M_{mol}} \int_0^\infty d\omega \frac{Z(\omega)}{\omega} n(\omega), \tag{11}$$

$$K_{av} = \frac{6}{4} \int_0^\infty d\omega Z(\omega) \coth(\hbar\omega\beta/2), \tag{12}$$

$$\Lambda^2 = \frac{4K_{av}}{3\hbar\gamma(0)} - \frac{1}{\gamma^2(0)},$$

$$2W(Q) \equiv \frac{\hbar Q^2}{4M_{mol}} \int_0^\infty d\omega \frac{Z(\omega)}{\omega} \coth(\hbar\omega\beta/2). \tag{13}$$

Notice that both the multiexcitation and incoherent contributions as well as those regarding single-particle dynamics are added to the model scattering laws and do not involve additional parameters to be refined during the fitting. Also, the ratio of quasielastic to inelastic intensities is governed by the values of the oscillator strength H_Q of Eq. (5), for which no closed form (sum-rule) expression is available because of the highly damped nature of the motions, although it is expected to show oscillations which are in phase with those of the $S(Q)$ static structure factor.

In order to compare the present results with those reported by Teixeira *et al.* [3], the intensities for the liquid were also analyzed using the oversimplified model

$$I_{obs}(Q,\omega) = \left[A\delta(\omega = 0) + B \frac{\omega}{1 - \exp(-\hbar\omega\beta)} \times \frac{\Gamma}{(\omega^2 - \omega_s^2)^2 + \omega^2\Gamma^2} \right] \otimes R(Q,\omega), \tag{14}$$

where $\delta(\omega = 0)$ once folded with the experimental resolution is used to mimic all the quasielastic processes and the second term is a damped harmonic oscillator with frequency ω_s and decay constant Γ. Notice that the relative weights of the elastic and inelastic contributions are given by the A, B constants which are considered as free parameters.

III. RESULTS

A comparison of two sets of corrected spectra corresponding to the hot solid and liquid, covering a representative set of momentum transfers below 3 Å^{-1}, is shown in Fig. 2, for an interval of energy transfers which covers more than 90% of the spectral power within the referred

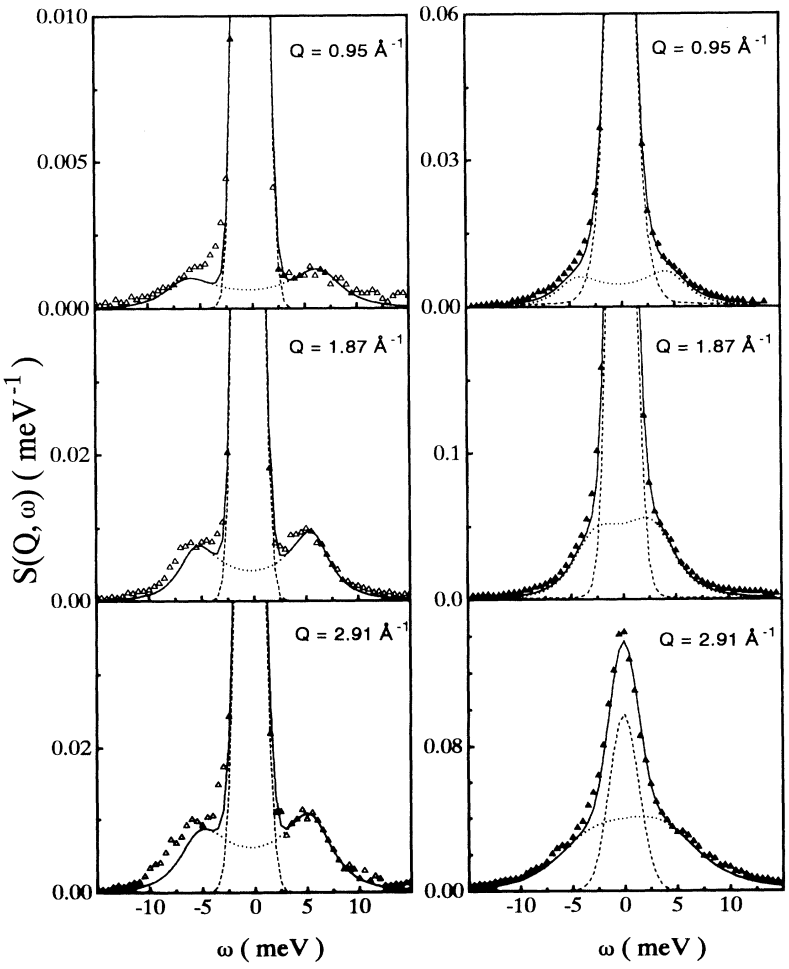

FIG. 3. A comparison between the experimental intensities (symbols) for ice (left) and liquid water (right), and the approximation in terms of the model functions given by Eqs. (2)–(4) (solid lines). The elastic (for the solid) or quasielastic (for the liquid) intensities are shown by the dashed lines. The inelastic response given by Eq. (5) is depicted by the dotted line. Values for the momentum transfers are given in the insets.

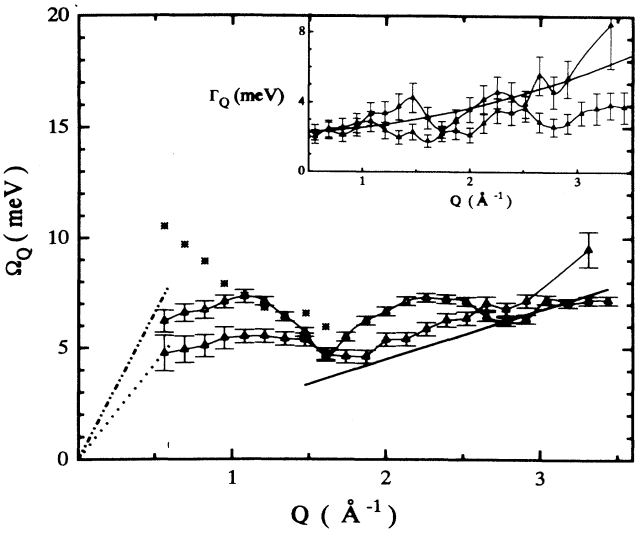

FIG. 4. Wave vector dependence of the renormalized excitation frequencies Ω_Q for solid (open symbols) and liquid water (filled symbols). The dash-dotted and dotted lines represent the adiabatic sound velocities for solid and liquid, respectively. The solid line drawn from 1.5 Å$^{-1} \leq Q \leq 3.5$ Å^{-1} corresponds to the ideal gas limit for the liquid (see text). The asterisks show the fitted values for the ω_s frequencies resulting from the analysis of the liquid spectra in terms of the simplified expression given by Eq. (14). The inset shows the Γ_Q linewidth factors for ice (open symbols) and liquid (filled symbols). The curve drawn through the data corresponds to a quadratic plus a constant term (see text).

range of wave vectors. The most remarkable difference is the absence of any finite-frequency feature identifiable by visual inspection for energy transfers below 15 meV in the melt, although the line shapes become clearly non-Lorentzian. Apart from some spurious effects, already mentioned in the preceding section, which lead to some asymmetries in the spectra and are especially severe for the lowest intense spectra [e.g., at $Q = 0.82$ Å^{-1} corresponding to a momentum transfer far below the first peak of $S(Q)$], the spectra of the liquid exhibit a sizable inelastic contribution which, although centered at zero frequency, covers a range of energy transfers far wider than that covered by purely stochastic motions and accounted for by the terms $S^0(Q,\omega)$ and $S_I(Q,\omega)$ of Eqs. (3) and (4), i.e., the quasielastic scattering from long-range translational diffusion and single-molecule reorientations. In contrast, the solid shows well-defined excitation peaks with maxima located about 5 meV not evidencing, for the selected set of momentum transfers, any strong dispersive behavior. The physical soundness of the model used to analyze the intensities can be estimated from Fig. 3, where the different contributions to the observed intensity are displayed for some selected values of momentum transfer. It appears that $I_{obs}(Q,\omega)$ is rather well reproduced in ice as well as in water, evidencing in the latter the importance of inelastic scattering with respect to the purely quasielastic response.

The wave vector dependences of the parameters describing the inelastic response for the solid and liquid samples are plotted in Fig. 4 as the renormalized frequencies Ω_Q and the values of the damping (or linewidth) factors Γ_Q. Again it is worth stressing that such frequencies must be interpreted as average (or effective) quantities, the meaning of which is the very same as $\omega_{max}(Q)$ derived from the frequency position of the maximum of the longitudinal current spectrum $J_l(Q,\omega)$ [i.e., the expression given in Eq. (5) ensures that Ω_Q corresponds to the maximum of $\omega^2 S(Q,\omega)$]. Under such circumstances it becomes clear that for wave vectors well within the kinematic range accessible to neutron spectroscopy or computer molecular dynamics such frequencies correspond to a maximum of a manifold of distinct excitation lines, although they are expected to show some phase relationships with the static structure factors. On the other hand, towards the hydrodynamic limit, the Q dependence of such frequencies is expected to approach the linear dispersion regime characteristic of hydrodynamic sound [19]. As can be seen from the referred Fig. 4, both in the solid and the liquid the "dispersion curves" stand somewhat below such a limit, going to a flat maximum located at about $Q_p/2$, with Q_p being the wave vector where $S(Q)$ attains its first maximum. In the case of the solid, the frequencies above some 2 Å^{-1} oscillate around an average value of about 7 meV which corresponds to the frequency of the first intense peak in the vibrational density of states [5], normally assigned to a transverse acoustic (TA) mode [20], whereas in the liquid these continue increasing with Q in a linear fashion, with a slope not far from that expected for the ideal gas behavior $(Q^2/M_{mol}\beta)^{1/2}$ [$\beta = (k_B T)^{-1}$] as calculated from the effective mass given above (i.e., better agreement would obviously be achieved by using a slightly smaller value for M_{mol}).

To illustrate the importance of a proper account of the quasielastic intensities, the results of analyzing the liquid data with Eq. (14) are also shown in the graph. As can be seen, lumping together all the quasielastic, incoherent, and multiexcitation intensities into a single, elastic term has rather dramatic consequences since the derived values for the oscillator frequencies ω_s are raised to considerably higher frequencies. As a matter of fact, the value of 10.32 meV corresponding to the ω_s parameter for the lowest explored momentum transfer (0.56 Å^{-1}) becomes close to that of $\approx$ 12 meV reported in Ref. [3] for $Q = 0.55$ Å^{-1}. At higher momentum transfers the values of ω_s are substantially decreased and are comparable to those of Ω_Q above 1 Å^{-1}, that is, within the region where most of the quasielastic scattering is of coherent nature leading to linewidths which are increasingly narrowed up to Q_p [i.e., the maximum of $S(Q)$]. It seems then clear that the approximation used in Ref. [3] to analyze the data has to be bounded to wave vectors above some 0.8 Å^{-1} where the quasielastic processes are confined to a narrow region of momentum transfers (de Gennes narrowing), and therefore can be represented by a single elastic component.

To check the physical meaning of the derived frequencies, recourse was made to a comparison of such quantities with the lower even frequency spectral moments

calculated from

$$\mu_n = \int_{E_{min}}^{E_{max}} d\omega\ \omega^n\ S_{coh}(Q,\omega), \tag{15}$$

$$S(Q) = \mu_0, \tag{16}$$

$$\langle\omega_0^2\rangle = \frac{\mu_2}{S(Q)}, \tag{17}$$

$$\langle\omega_l^2\rangle = \frac{\mu_4}{\mu_2}, \tag{18}$$

where $E_{min,max}$ are the limits imposed by the neutron kinematics, and were set to $\pm$ 20 meV in the explored range of momentum transfers. As is well known, the zeroth-order moment provides an approximate value of the static structure factors due to the limited range of energy transfers. This is reported in the upper frames of Fig. 5 for ice and liquid heavy water. In both cases a good agreement with the corresponding quantity obtained from diffraction measurements is found. The lower frames of Fig. 5 provide a comparison between the calculated frequency moments and the frequency of the damped oscillator derived by the fitting procedure. First and foremost, it is worth remarking the close proximity between the curves giving the frequency dependence of Ω_Q and $\omega_{max}(Q)$, taken as that corresponding to the first extremum in the longitudinal current autocorrelation as calculated from $S_{coh}(Q,\omega)$, which in the case of the melt will include a small contribution from the quasielastic wings, which accounts for the relatively larger difference between these two frequencies seen in the liquid than in the solid, where up to at least $Q_p/2$, they are basically coincident. On the other hand, $\omega_0(Q)$, the square root of $\langle\omega_0^2\rangle$, turns out to be smaller than Ω_Q within the whole wave vector range, the two being in much better agreement at the smallest Q values where in fact one may expect to approach the hydrodynamic limit, $\lim_{Q\to 0}\langle\omega_0^2\rangle = Q^2 v_T^2$, where v_T is the adiabatic sound velocity. At large wave vectors the square roots of the second and fourth reduced frequency moments are found to follow the ideal gas behavior.

The low-frequency $c_0(Q)$ and high-frequency $c_\infty(Q)$ limits of the sound velocity can be derived from the values of the frequency moments as follows [21]:

$$c_0^2(Q) = \frac{\gamma\langle\omega_0^2\rangle}{Q^2} \propto \frac{\gamma/(\beta M_{mol})}{S(Q)},$$

$$c_\infty^2(Q) = \frac{\langle\omega_l^2\rangle\ \beta\ M_{mol}}{Q^2} \propto \frac{c_{11}(Q)}{\rho}, \tag{19}$$

where γ stands for the ratio of specific heats, $c_{11}(Q)$ is the infinite-frequency longitudinal modulus, and ρ is the density of the system. In principle these expressions are

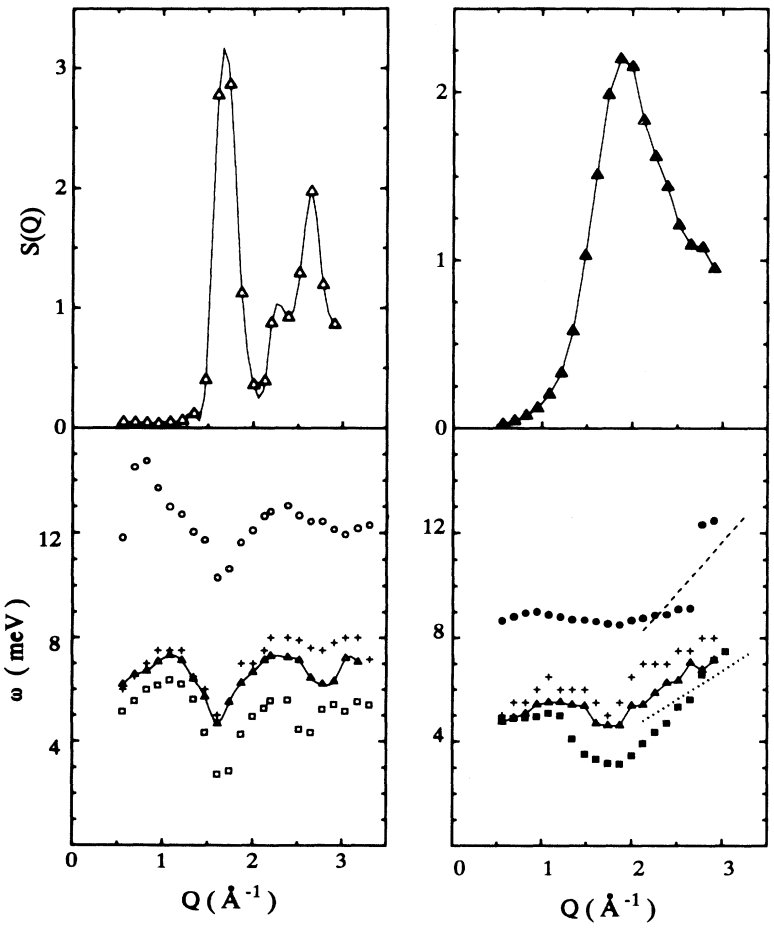

FIG. 5. Frequency moments of the model $S(Q,\omega)$ structure factors arising from fits to the experimental intensities and calculated from Eq. (14). The upper part of the graphs shows the zero-frequency moments of the response functions for ice (left) and liquid water (right), and can be compared with static structure factors $S(Q)$. The lower frame compares the wave vector dependence of the renormalized frequency Ω_Q (triangles) with that corresponding to the maximum of the longitudinal current correlation, $\omega_{max}(Q)$ (crosses), as well as with the square roots of the reduced second (squares) and fourth (circles) moments, $\langle\omega_0\rangle$ and $\langle\omega_l\rangle$, respectively [Eqs. (16) and (17)], of the scattering law.

valid for a monoatomic fluid; for a molecular system they can be used to describe the overall center of mass motion [9]. In simple liquids both $c_0(Q)$ and $c_\infty(Q)$ are found to be constant in the hydrodynamic wave vector range (i.e., up to say 0.1–0.3 Å^{-1}) and to fall to nearly zero at $Q = Q_p$. A comparison between $c_0(Q)$, $c_\infty(Q)$, and the phase velocity Ω_Q/Q derived from the analysis of experimental data is shown in Fig. 6. As is apparent, this latter velocity is found to sit between the two curves marking the zero- and infinite-frequency cases. It is worth noting that it shows a monotonous decrease in going from $Q = 0.56$ Å^{-1} to a flat minimum at $Q = Q_p$, and in any case remains very close to the zero-frequency limit. This behavior is in marked contrast with previous experimental [3] and computer simulation findings [2,22] which showed a strong increase of the sound velocity in going from low to intermediate Q's, being already more than two times bigger than the hydrodynamic value at $Q = 0.3$ Å^{-1}. Notice, however, that if the ω_s frequencies shown in Fig. 4 are converted to excitation phase velocities, a value of 2800 ms^{-1} is found for $Q = 0.56$ Å^{-1}, and can be compared with that of 3400 ms^{-1} derived from data shown in Ref. [3] for $Q = 0.55$ Å^{-1}.

The only other remarkable feature of the liquid and polycrystal spectra is found at wave vector larger than 2.7 Å^{-1} and it appears as an envelope of excitations located within the range of energy transfers 22 meV $\leq \hbar\omega \leq$ 30 meV, i.e., also within the so called translational band. The intensity of these bands turned out to be large enough to be resolved from the background. An illustrative example is reported in Fig. 7(a), whereas Fig. 7(b) shows the Q dependence of the corresponding characteristic frequencies, obtained from the maxima of $\omega^2 I_{obs}(Q,\omega)$. The interesting point to be stressed here is the strict analogy of the observed Q dependence of the characteristic frequency with that found in a previous independent experiment on polycrystalline ice Ih at $T = 88$ K carried out by a triple-axis spectrometer and reported in Ref. [8]. There, a well-defined sharp excitation peak was found within a similar range of momentum transfers similar to the one reported in the present work. The shape and characteristic frequency of this peak, at large Q, allows us to unambiguously identify it with the same peak which gives rise to a well-defined feature in the density of states, usually referred to as a transverse optic (TO) [5,7,20]. The following argument has been brought forward, from considerations about the lattice constants [8], to explain the presence of such a band: since two of the dimensions of the primitive cell of hexagonal ice Ih are not far from being one-half of the third, the zone boundary for the in-plane directions is found to be in close proximity to the lower harmonics corresponding to

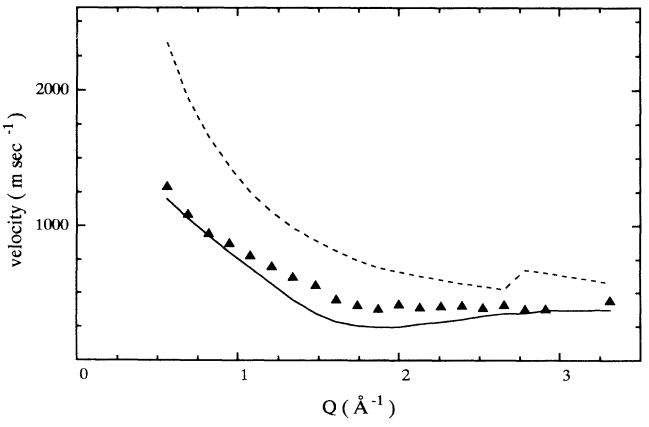

FIG. 6. Low-frequency $c_0(Q)$ (solid line) and high-frequency (dashed line) $c_\infty(Q)$ limits of the phase velocities of the excitations as calculated according to Eq. (19). The solid triangles stand for the values of the actual magnitude as calculated from the Ω_Q/Q.

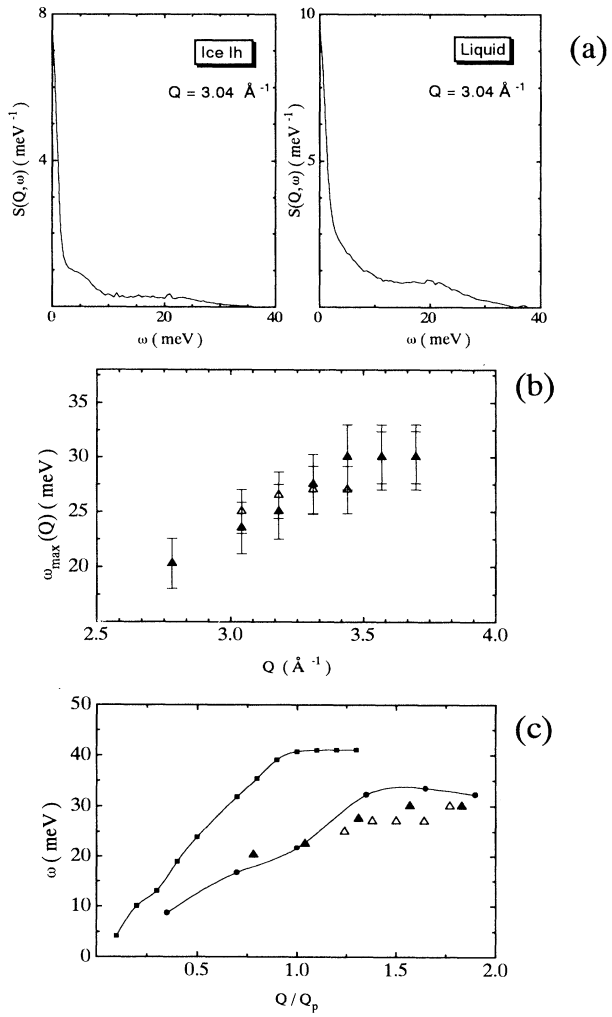

FIG. 7. Wave vector dependence of the frequencies of the higher-energy manifolds. (a) Two representative spectra showing the shapes of these higher-frequency bands for the solid (left) and liquid (right). (b) Wave vector dependence of their average frequencies. Open triangles refer to ice and filled ones to liquid phase. (c) A comparison of the frequencies after rescaling their characteristic wave vectors (see text), with the apparent dispersion observed for the harmonic crystal (filled squares) and for results arising from molecular dynamics calculations for the liquid (filled circles). Open and solid triangles have the same meaning as in (b).

the out-of-plane directions. As a result, the wave vectors corresponding to the observed excitations could be displaced by subtraction of Q_p down to the first Brillouin zone. Such a procedure which seems entirely justified for ice but has to be taken with care when applied to the liquid has been employed with the present data, and the results are compared with those calculated for the harmonic polycrystal [7], and those arising from computer MD simulations in the melt (Sastry *et al.* [2]) in Fig. 7(c). The most interesting aspects of this comparison concern both the close proximity of data for water and the hot ice, as well as the closeness of the experimental points to those derived from MD simulations. Further comments on this particular point are deferred to the next section.

IV. DISCUSSION AND CONCLUSIONS

The most remarkable finding of the present study is perhaps the close similarity of the inelastic response of water at low frequencies (i.e., below some 20 meV) with that observed by neutron scattering and computer MD simulations in some other molecular liquids [9,11]. In particular, the measured excitation frequencies come rather close to those found for a related, hydrogen-bonded liquid [9], namely, methanol, where both the shape and maximum frequencies of the curves giving the wave vector dependence of the second and fourth reduced frequency moments are reminiscent of those found in the present study. For a unique interpretation of the physical processes underlying the measured spectra, the experimental conditions have been chosen in such a way that the wave vector dependent spectra, for momentum transfers below 1 Å^{-1}, could be detected only in the region between zero and 20 meV, since both the intensity of those excitation lines above 20 meV turns out to be too low to enable a sensible extraction of the signal from the background noise and the width of the zero-frequency line remains confined below the first 5 meV. We believe that only in this spectral range does the analysis of the inelastic part in terms of a single damped oscillator have a sound basis and the extension of acousticlike excitations from the $Q \rightarrow 0$ limit is reasonable. The resulting values of the characteristic frequencies and velocities give strong support to this assumption, being corroborated by the comparison with the results found in other molecular liquids [9,11]. We are aware of the fact that our findings are in contrast with early neutron scattering data [3] and with a substantial number of MD simulations [2,10] performed with different potential models, which show "dispersion branches" reaching some 33 meV at Q values around Q_p. The origin of such a discrepancy has to be found in the increasing importance arising from "nonacoustic" contributions in the spectral region beyond 20 meV, emphasized by the fact that the dispersion curves are always constructed by reporting the maximum frequency of the longitudinal current spectrum $J_l(Q,w)$. The nature of this high-frequency excitation, discussed in a previous work [7,9] as well as in a MD study by Sciortino and Sastry [2], can be envisaged, for example, in collective and/or single-molecule reorientation processes and other excitation modes which show an optical-like character.

The curves showing the Q dependence of the excitations for liquid water shown in Figs. 4 and 5 [Ω_Q and $\omega_{max}(Q)$] can be favorably compared with those calculated from a treatment carried out in terms of the Mori-Zwanzig projection operator technique applied to a two-component dynamical variable which accounts for the density fluctuations of hydrogen and oxygen as reported in Ref. [22], or that derived from simulation means by Wojcik and Clementi [2], although in this latter case, both the higher temperature of the system employed (i.e., larger hydrodynamic sound velocity) and the possible inadequacies of the model potential used lead to maximum frequencies about Q_p some 40% higher than the ones reported here.

The reason most of the observed intensity in the spectrum of the hot polycrystalline solid arises from the transverse acoustic modes which give rise to the first intense band in the $Z(\omega)$ vibrational frequency distribution can be easily understood from consideration of the strong intensity of this band in comparison with that regarding longitudinal sound (LA) as evidenced from experiments [5] or calculation [7] results. As a matter of fact, as shown in our previous paper [7], the dispersion behavior of those excitations grouped under the LA branch becomes rather difficult to follow once a polycrystalline average of the single-crystal dynamic structure factor is performed (see Fig. 3 of Ref. [7]). Notice, however, that the presence of two dispersion branches of optical origin which cross the LA curves and have frequencies comparable with the maximum ones of the TA modes implies that the observed excitation envelopes are by no means of a pure acoustic character. At this point it is also interesting to note that the experimental frequencies regarding the dispersion of polycrystalline ice *Ih* at 90 K [4] are also confined below 18 meV, whereas some of the reported curves from MD simulations in the liquid reach values as high as 33 meV [2,22]. As discussed in previous work [7,8], the origin of such steep dispersion is better ascribed to the buildup of intensities arising from modes of optical origin, an explanation which is also supported by the fact that such large frequencies coincide with the ones commonly referred to as transverse optic for most of the ice polymorphs [5,7] as well as from the observation that the intensity of the peaks characteristic of such rapid dispersion goes to zero for wave vectors above Q_p.

Because of the inability of the neutrons to couple with shear-mode (transverse acoustic) excitations in the liquid, the observed inelastic scattering in the melt cannot be attributed to transverse excitations, even if their characteristic velocities, as estimated in a recent contribution to the present debate by Sciortino and Sastry [2] as $\approx 1300\ \text{m sec}^{-1}$, come very close to that of hydrodynamic sound [19]. This can be readily understood if one considers the effects of orientational averaging on the sound velocity characteristic of the parent (hexagonal) crystal, for which the orientationally averaged speed of sound can be calculated using experimental, angle-dependent data for the single crystal given by Gagnon *et al.* [19]. Then, estimates of the effective speed for an isotropic continuum, something applicable to the amorphous or quenched liq-

uid (see Sciortino and Sastry [2]) cases, are given by $3/v_{eff}^3 = 1/v_l^3 + 2/v_t^3$ where $v_l = \int_0^{\pi/2} d\phi\ v_l(\phi)\ \sin(\phi)$ is the directionally averaged longitudinal sound velocity, ϕ stands for the angle between the crystal c axis and the wave vector of the sound waves, and v_t is the transverse sound speed. The numerical values for the averaged longitudinal and transverse velocities are 3914 m sec^{-1} and 1995 m sec^{-1}, respectively, giving a value for the effective speed v_{eff} some 240 m sec^{-1} close to that of the transverse waves, thus becoming too close to be distinguished from the shear-wave velocity, unless additional data are available.

The absence of well-resolved inelastic peaks in the liquid even at this temperature close to the freezing point was not unexpected because of the high anharmonicity of the molecular motions as was recently evidenced by its relatively large contribution to the specific heat [5], as well as from the loss of the long-range order of the oxygen lattice. An indication of both effects can be seen by the Q dependence of the Γ_Q coefficients shown in Fig. 4, where it can be seen that those regarding the liquid increase with wave vector faster than those of the solid, although the relatively large errors hinder any quantitative conclusion about its explicit Q dependence. Moreover, caution has to be exercised when analyzing the behavior of the linewidth parameter since, as mentioned above, a rather substantial part of its magnitude arises from the fact that different sets of excitations are being analyzed with only one damped harmonic oscillator function. A way to estimate the relative importance of the two (homogeneous and heterogeneous) broadenings would be considering the hydrodynamic limit, $\lim_{Q\to 0} \Gamma_Q$, which gives some measure of the heterogeneous contribution. From the inset shown in Fig. 4, it can be seen that such a limit is found to be of the order of 2 meV for both liquid and solid, a value comparable with the width of the TA band in most of the experimental [5] or computational [7] estimates of this magnitude measured at low temperatures. Such a limiting value thus enables a qualitative understanding of the wave vector dependence of the oscillator widths arising from a contribution with a weak Q dependence arising from the heterogeneous term, and a Q-dependent term which for the liquid at low wave vectors is expected to follow a quadratic behavior in Q with a coefficient given in terms of viscous and thermal conductivity contributions to the damping, which, from data plotted in the inset of the figure, yields a value of ≈ 0.39 meV Å^2.

The Q dependence of the phase velocities of the excitations shown in Fig. 6 is in stark contrast with similar graphs regarding MD results [2,10], where an increase in velocity with wave vectors up to $\approx Q_p/2$ and a subsequent decrease is found. The origin of such a feature has, again, to be attributed to the increasing importance of intensities arising from nonacoustic contributions to the calculated $J_l(Q,\omega)$ profiles and evidenced in our previous work [9,7] as well as pointed out in a recent contribution to this topic by Sciortino and Sastry [2], where from simulational means it was found that pure sound-wave excitations in water are confined to frequencies below 6.2 meV, something which is substantiated in the present study (see Fig. 4).

The wave vector dependence of the excitations within the *optic* manifolds shown in Fig. 7 corroborates our previous results on low-temperature ice [8], and also gives further support to the interpretation of the steep dispersion put forward in Ref. [7]. The reason such excitations were not directly observed within the first Brillouin zone (or its equivalent to the liquid, that is, below Q_p) is easily found in the kinematics of the present experiment (as shown in Fig. 1, the required range of energy transfers is bounded above 1 Å^{-1}), as well as in the weak inelastic intensities which basically follow a Q^2 law within such a region. Although the procedure of rescaling the Q vectors in the liquid case cannot be justified in full, the fact that the characteristic times of those excitations are rather short on a molecular scale $\approx 10^{-13}$ sec serves to locate them on a time window where the description of liquid dynamics within the instantaneous normal modes approach becomes adequate [23]. Such a fact in conjunction with the close similarity of the static short-range structure in ice *Ih* and water close to freezing [24] can therefore serve to understand the closeness of the dynamic response of the two systems at these time and length scales.

Finally, it would be interesting to attempt to relate the spectrum of excitations seen in the solid with quantities encompassing the liquid dynamics following steps equivalent to those employed for the treatment of simple crystal structures in terms of some variants of the density functional theory of freezing [25]. Although application of such treatments to liquids composed by nonspherical particles have been hindered by the requirement of correlation functions of higher order than the direct correlation function, such as triplet correlations, very recent advances in the interpretation of neutron diffraction data of heavy water in terms of correlations beyond the pair approximation [26] constitute a promising step in this direction.

In summary, the present paper provides experimental evidence indicating that, at temperatures slightly above the melting point, heavily damped sound waves can propagate in water at wavelengths much shorter than the ones concerning the hydrodynamic regime. The corresponding velocities of propagation are found to be close to those one would expect from a continuation for large wave vectors of the linear dispersion law, in stark contrast with previous experimental and computer simulation findings. In particular, the results given here, albeit at odds with those of Teixeira *et al.* [3], provide an explanation for the apparently anomalous dispersion reported there as arising from an incomplete modeling of the low-frequency (quasielastic) intensities which, as shown in Fig. 4, becomes important at momentum transfers below some 0.8 Å^{-1}. Also notice that the lower temperature explored in the present experiment bounds the intensities arising from the quasielastic wings to energy transfers comparable with the instrumental resolution, and that both counting statistics and resolution in energy transfers are substantially improved with respect to those achieved in Ref. [3]. In consequence, the analysis of these new neutron scattering data allows us to conclude that the higher-frequency excitations reported in

previous works for water at room temperature can be explained neither by an increase of the sound velocity (highly positive dispersion law) nor by the presence of a new mode propagating through hydrogen-bond patches ("fast sound"), but by the fact that the dynamical response of water contains contributions from a richer variety of physical processes as reorientational relaxations, optical-like modes of excitations, and so forth. Therefore a deep examination of the whole inelastic spectrum (extending to some 40 meV) would certainly require a much more elaborate model than the simple damped harmonic oscillator. From the present analysis it seems now clear that the fingerprints of sound propagation in water at length scales comparable with intermolecular separations are confined to frequencies well below 10 meV approaching the hydrodynamic limit in a way common to other molecular liquids [9]. In fact, the wave vector dependence of the parameters used herein to model the physical processes responsible for the inelastic scattered intensity in liquid water is found to be akin to that derived for other molecular systems and the shape of such curves is somewhat reminiscent of that observed in simple (monoatomic) liquids. Perhaps the most distinctive feature regarding the spectra of water concerns the appearance, at relatively large wave vectors, of a second manifold of excitations clearly identifiable with collective out-of-phase ("optical") motions.

ACKNOWLEDGMENTS

This work has been supported in part by EEC Grant No. SCI-CT91-0714. M.A. would like to thank Royal Institute of Technology for kind hospitality and the European Community for support with a Science Programme grant. The authors are grateful to M.A. Ricci for her kind assistance during the experiment and encouraging discussions. Thanks are also given to H.E. Smorenburg, A. Mellergård, and P. Zetterström for very helpful comments.

[1] A. Rahman and F.H. Stillinger, Phys. Rev. A **1**, 368 (1974).

[2] Such a suggestion was stated in J. Bosse, G. Jacucci, M. Ronchetti, and W. Schirmacher, Phys. Rev. Lett. **57**, 3277 (1986). Computer molecular dynamics calculations at different levels of sophistication were carried out by, among others, R.W. Impey, P.A. Madden, and I.R. McDonald, Mol. Phys. **46**, 513 (1982); M. Wojcik and E. Clementi, J. Chem. Phys. **85**, 6085 (1986); S. Sastry, F. Sciortino, and H.E. Stanley, *ibid.* **95**, 7775 (1991); F. Sciortino and S. Sastry, *ibid.* **100**, 3881 (1994).

[3] J. Teixeira, M.C. Bellisent-Funel, S.H. Chen, and B. Dorner, Phys. Rev. Lett. **54**, 2681 (1985).

[4] B. Renker, Phys. Lett. **30A**, 493 (1969). Also reproduced in *Phonon Dispersion Relations in Insulators*, edited by H. Bilz and W. Kress (Springer, Berlin, 1979), p. 187.

[5] D.D. Klug, E. Whalley, E.C. Svensson, J.H. Root, and V.F. Sears, Phys. Rev. B **44**, 841 (1991).

[6] A recent account on total (i.e., integrated in energy) diffuse scattering from hexagonal ice is given in J.C. Li, V.M. Nield, D.K. Ross, R.W. Whitworth, C.C. Wilson, and D.A. Keen, Philos. Mag. B **69**, 1173 (1994).

[7] A. Criado, F.J. Bermejo, M.García-Hernandez, and J.L. Martínez, Phys. Rev. E **47**, 3516 (1993).

[8] F.J. Bermejo, E. Frikee, M. García-Hernandez, J.L. Martínez, and A. Criado, Phys. Rev. E **48**, 2300 (1993).

[9] J. Alonso, F.J. Bermejo, M. García-Hernandez, J.L. Martínez, W.S. Howells, and A. Criado, J. Chem. Phys. **96**, 7696 (1992); Phys. Lett. A **172**, 177 (1992).

[10] U. Balucani, G. Ruocco, M. Sampoli, A. Torcini, and R. Vallauri, Chem. Phys. Lett. **209**, 408 (1993).

[11] For an experimental study regarding the excitations in liquid deuterium close to melting see F.J. Bermejo, F.J. Mompean, M. García-Hernandez, J.L. Martínez, D. Martin, A. Chahid, G. Senger, and M.L. Ristig, Phys. Rev. B **47**, 15097 (1993). For those regarding a molecular simple liquid see M. García-Hernandez, J.L. Martinez, F.J. Bermejo, A. Chahid, and E. Enciso, J. Chem. Phys. **96**, 8477 (1992), and for a dense dipolar liquid see F.J. Bermejo, J.L. Martinez, D. Martin, M. García-Hernandez, and F.J. Momplan, J. Chem. Phys. **95**, 5287 (1991).

[12] F.J. Bermejo, F. Batallán, E. Enciso, M. García-Hernandez, J. Alonso, and J.L. Martínez, Europhys. Lett. **12**, 129 (1990).

[13] F.G. Bischoff, Ph.D. thesis, Rensselaer Polytechnic, 1970, available from University Microfilms, Ann Arbor, MI, order No. 70-19,931; J.R.D. Copley, Comput. Phys. Commun. **7**, 289 (1974); J.R.D. Copley, P. Verkerk, A.A. van Well, and H. Fredridkze, *ibid.* **40**, 337 (1986), and references therein.

[14] B. Fåk and B. Dorner, Institut Laue Langevin (Grenoble, France), Technical Report No. 92FA008S, 1992 (unpublished).

[15] V.F. Sears, Can. J. Phys. **44**, 1299 (1966); **45**, 237 (1966).

[16] J. Teixeira, M.C. Bellisent-Funel, S.H. Chen, and A.J. Dianoux, Phys. Rev. A **31**, 1913 (1985). Additional results regarding the translational linewidths can be found in J.J. Ullo, Phys. Rev. A **36**, 816 (1987).

[17] V.F. Turchin, *Slow Neutrons* (Israel Programme for Scientific Translations, Jerusalem, 1965), p. 181.

[18] S.W. Lovesey, *Theory of Neutron Scattering from Condensed Matter* (Oxford Science Publications, Oxford, 1986), Vol. 1, Sec. 4.8.

[19] Sound velocities and elastic constants for ice *Ih* were taken from R.E. Gagnon, M.J. Clouter, and E. Whalley, J. Chem. Phys. **89**, 4522 (1988); **92**, 1909 (1990), and the value of the orientationally averaged velocity for ice *Ih* at these thermodynamic conditions was found to be 1990 $\mathrm{m\,sec^{-1}}$. The sound velocity data for heavy water at the temperature of interest were found to be $\approx 1300\ \mathrm{m\,sec^{-1}}$, from O. Conde, J. Teixeira, and P. Papon, J. Chem. Phys. **76**, 3747 (1982).

[20] The assignment of peaks follows that used by H.J. Prask, S.F. Trevino, J.D. Gault, and K.W. Logan, J. Chem. Phys. **56**, 3217 (1972), and should be considered as semi-

quantitative since a clear separation between translations and rotations can only be pursued at very low Q values [7].

[21] J.P. Boon and S. Yip, *Molecular Hydrodynamics* (McGraw-Hill, New York, 1980).

[22] M.A. Ricci, D. Rocca, G. Ruocco, and R. Vallauri, Phys. Rev. A **40**, 7226 (1989).

[23] See, for instance, M. Cho, G.R. Fleming, S. Saito, I. Ohmine, and R.M. Stratt, J. Chem. Phys. **100**, 6672 (1994), and references therein. An application to a real liquid (cesium) is given in R. Vallauri and F.J. Bermejo Phys. Rev. E **51**, 2645 (1995).

[24] A.K. Soper and M.G. Phillips, Chem. Phys. **47**, 107 (1986).

[25] M. Ferconi and M.P. Tosi, Europhys. Lett. **14**, 797 (1991).

[26] A.K. Soper (unpublished data).